P2.3 SUMMERTIME LOW-LEVEL JETS OVER THE HIGH LATITUDE ARCTIC OCEAN

Douglas O. ReVelle
Earth and Environmental Sciences Division, Los Alamos National Laboratory
E. Douglas Nilsson
Department of Meteorology, Stockholm University

1. INTRODUCTION AND OVERVIEW

1.1 AOE-96 (Arctic Ocean Expedition)

Modeling of the Arctic Ocean atmospheric boundary layer (ABL) is in some ways similar to modeling of the nocturnal boundary layer over land in middle and high latitudes. The key to understanding the Arctic boundary layer is the tendency for strong static stability of the air over most of the year. The underlying surface that can be relatively warm, with temporally and spatially changing leads or ice flows creates an environment that is challenging to model. The International Arctic Ocean Expedition in 1991 (IAOE-91) greatly improved our understanding of the Arctic PBL characteristics (Nilsson, 1996), formation and decay of fogs and related phenomena (Nilsson and Bigg, 1996), i.e., gravity waves, intermittent turbulence, etc.

During the 3 month long Arctic Ocean Expedition (AOE-96) to the North Pole in the summer of 1996 an enormous amount of data was collected on the Arctic ABL. Basic observations include rawinsonde launches, aerosol and radiation data from helicopter flights, LIDAR and SODAR measurements, radiation and heat budget data (Nilsson et al., 1997), fog microphysics, aerosol physics and chemistry, etc. The data set includes many case intensive periods and also a 5 day ice-camp. Numerous details have been now been analyzed (Leck et.al., 2001, Bigg, Leck and Nilsson, 2001, Nilsson and Barr, 2001, Nilsson and Rannik, 2001, Nilsson, Rannik and Hakansson, 2001, etc.). Among the processes measured was a low-level wind maximum, the low-level jet (LLJ) present is some 2/3 of all rawinsonde soundings during AOE-96. Although numerous LLJ studies have been made over continental surfaces, few studies have been made over broad ocean regions. Some recent research contributions on LLJ's in the polar oceans can be found however in Andreas et. al. (1995, 2000). With the presence of low-level temperature inversions extending over broad polar oceanic regions, it is not surprising that these LLJ's are so common. Cumulative estimates from the work of Andreas and colleagues and from those of Nilsson and colleagues are that these LLJ's occur during about 60-80 % of all of the soundings taken during these various polar oceanic field expeditions.

Corresponding author address: Douglas O. ReVelle, P.O. Box 1663, MS J577, EES-2, Los Alamos National Laboratory, Los Alamos, New Mexico 87545: e-mail: revelle@lanl.gov

1.2 Boundary Layer Processes, Low-Level Jets and One-Dimensional Modeling:

Numerous physical processes occur in the atmospheric surface and planetary boundary layer. These range from transient, intermittent bursting events (ReVelle, 1993, Van de Wiel et. al, 2002a, 2002b, 200c) to organized mesoscale wind jets such as the low-level jet (see for example Blackadar, 1957, Thorpe and Guymer, 1977, Gill, 1982, ReVelle, Logsdon and Liu, 1990; Liu and ReVelle, 1992; ReVelle and Liu, 1992, Banta et. al, 2002, etc.). Atmospheric gravity (buoyancy) waves (Holton, 1992) from a variety of sources are also observed as well for regions of surface stability (Sorbjan, 1989). Since turbulent fluids can radiate gravity waves and large amplitude gravity waves can break and produce turbulent regions (Kundu, 1990), it is not at all surprising to find these two physical processes coexisting. Simplified analytical and numerical models now exist that can capture some of the most essential physics in these processes (ReVelle, 1993, Van De Wiel et. al., 2002a, 2002b, 2002c, etc.). Enhanced surface ozone levels have also been found during both intermittent bursting episodes (ReVelle, 1993) and during LLJ's (Corsmeier et. al., 1997). This is also not too surprising since these two physical phenomena have also been indirectly linked (Thorpe and Guymer, 1977; ReVelle, 1993).

2. LOW LEVEL JET DYNAMICAL MECHANISMS

2.1 Low Level Jet Definitions:

2.1.1 Coriolis Force Representations

The proper representation of the Coriolis force/mass in the simplest coordinate system indicative of the physical process occurring is a problem that is common to Meteorology, with the outstanding numerical weather prediction example being the representation of the relevant forces acting on barotropic and baroclinic Rossby waves on a spherical planet (Holton, 1992). If the gradient of the

Coriolis parameter with latitude is not taken into account, such Rossby waves could not exist at all, yet they dominant the observable mid-levels of the atmosphere and are an essential element of middle latitude weather forecasting techniques. A similar situation may also occur for the low-level jet that we will now examine. The dynamical description of the resulting wind field depends fundamentally on whether a Cartesian or a spherical or other type of coordinate system description is utilized as will be shown below. This leads to the necessity of investigating the effects of utilizing an f plane, i.e., the Cartesian coordinate system description versus the Beta plane approximation, i.e., the spherical coordinate system description for the expected behavior of the LLJ. This aspect of the LLJ dynamics will be discussed next.

It should be admitted from the onset that our basic approach to this problem is from the standpoint of the relevant boundary layer physics rather than that of synoptic scale or of mesoscale meteorology. Thus, some additional critical aspects of the LLJ involving moisture convergence properties and meteorological storm development as well as the influence of mountains and steeply sloped terrain are not considered here (see for example, Ray, 1986). It is strongly felt that until the boundary layer part of this problem is adequately understood and more readily predictable, reliable analysis of the other significant parts of this problem are problematic at best. Similar comments have also been made about our ability to predict synoptic scale frontal passage near the Earth's surface for the same reason (Anthes, 1980).

We proceed to briefly review the proposed hypothetical processes associated with the classical and non-classical diurnal release of surface friction in the boundary layer, i.e., the inertial oscillation of the ageostrophic part of the total wind vector. This protype process seems to be most able to readily explain the summertime Arctic low-level jets that we have observed as we shall soon demonstrate. In this description, we have consistently replaced the length of night parameter with the time period over which z/L > 0, i.e. stability of the lowest part of the surface boundary layer with respect to the Monin-Oboukhov–Lettau length, L. We also replace the term "sunset" with the time of the onset of the period with z/L > 0 so that an equivalent explanation of the LLJ can be provided with the same set of dynamical equations.

2.1.2 f and Beta Plane Descriptions

The well known difference between the f plane and the Beta plane description of the Coriolis parameter, f can be represented for horizontal flow on a sphere as follows (Holton, 1992):

$$df/dt \equiv u\cdot\partial f/\partial x+v\cdot\partial f/\partial y+w\cdot\partial f/\partial z = v\cdot\partial f(y)/\partial y \qquad (1a)$$

$$f(y) = f_o+\beta\cdot y; \quad \partial f(y)/\partial y\equiv\beta \qquad (1b)$$

where

$f = f_o$ = constant in the f plane approximation

$f(y) = f_o+\beta\cdot y$ in the β plane approximation

For the f plane approximation to be sufficiently accurate, the wavelength associated with the LLJ in the north-south direction must be small compared to the radius of the Earth, r_e, i.e., $\lambda_y << r_e$. In addition, we have the added constraint that for the LLJ to be established its wavelength must be $\leq$ horizontal scale of a typical anticyclone, where its presence under the influence of inversion layers is readily established by radiational cooling during conditions of clear skies and light prevailing winds. Also, for the nocturnal continental case, we also must be in a regime where the inertial oscillation period τ_i ($\equiv 2\pi/f(y)$) must be comparable to the length of the night (or more generally for the Arctic low-level jet case for periods during which z/L is > 0). In fact, it can be shown for this case that the maximum wind ratio occurs when the length of night (or the period over which z/L > 0 for the summertime Arctic LLJ case) is exactly equal to the one half of inertial oscillation period.

The corresponding inviscid, coupled momentum equations for the LLJ can be written in the Beta plane approximation in terms of the prevailing synoptic scale geostrophic wind components for the east-west and north-south directions respectively $\{u_g, v_g\}$, which are assumed to be constants:

$$d/dt\{du/dt\} - v^2\beta - f(y)\cdot dv/dt + v\beta v_g = 0 \qquad (2a)$$

$$d/dt\{dv/dt\} + uv\beta + f(y)\cdot du/dt - v\beta u_g = 0 \qquad (2b)$$

where

$\beta = 2\Omega\cos\phi/r_e \cong 1.6\cdot10^{-11}$ m^{-1}s^{-1} in middle latitudes

$\Omega = 7.292\cdot10^{-5}$ s^{-1} = solid earth rotation rate

and

$$du/dt = -(1/\rho)\cdot\partial p/\partial x + f(y)\cdot v \qquad (2c)$$

$$dv/dt = -(1/\rho)\cdot\partial p/\partial y - f(y)\cdot u \qquad (2d)$$

These equations reduce in the f plane approximation, to the uncoupled, standard second order, ordinary differential equations with constant coefficients in the form:

$$d/dt(du/dt) + f_o^2(u-u_g) = 0 \qquad (3a)$$

$$d/dt(dv/dt) + f_o^2(v-v_g) = 0 \qquad (3b)$$

It is only these latter very simple equations that are normally solved in connection with the inertial

oscillation theory (Blackadar, 1957) of the LLJ dynamics.

If we now substitute into (2a,2b) and (3a, 3b) the decomposition of each of the wind components into geostrophic and ageostrophic parts respectively, i.e.,

$$u = u_g + u_{ag} \, , \, v = v_g + v_{ag} \qquad (4)$$

with the geostrophic part of the wind assumed constant for simplicity, we have the following coupled set of equations:

$$d/dt(du_{ag}/dt) + f^2(y)\cdot u_{ag} - \beta\cdot v_{ag}\cdot v = 0 \qquad (5a)$$

$$d/dt(dv_{ag}/dt) + f^2(y)\cdot v_{ag} + \beta\cdot u_{ag}\cdot v = 0 \qquad (5b)$$

that can be compared with the f plane approximation for constant geostrophic winds:

$$d/dt(du_{ag}/dt) + f_o^2\, u_{ag} = 0 \qquad (6a)$$

$$d/dt(dv_{ag}/dt) + f_o^2\, v_{ag} = 0 \qquad (6b)$$

A partial scale analysis (Holton, 1992) of equations (5a, 5b) which only examined changes of the correction terms involving β with latitude compared to the standard terms involving f_o in equations (6a, 6b) showed that southward of 30 deg latitude, significant correction factors can arise compared to the terms utilized in the standard set of equations commonly solved, i.e., (6a, 6b). This latitudinal behavioral change is proportional to $\cos\phi/\{\sin\phi\}^2$. This behavior was also independently confirmed in our analysis in Table 1 below and in addition was shown to be dependent on the magnitude of the geostrophic wind speed as well.

We can conclude immediately from our analysis above that the f plane approximation is completely justifiable for the analysis of the summertime Arctic LLJ at such high latitudes. This is because as $\phi \rightarrow 90$ deg, $\beta \rightarrow 0$, so that $f = f_o$ exactly at the earth's poles. At low latitudes, in complete contrast, it appears that the inclusion of β is a necessity to the complete formulation of the possible LLJ dynamical behavior. Thus, at such low latitudes, for LLJ's like those observed consistently in Koorin in Australia (Malcher and Kraus, 1983, Brook, 1985) which have anomalously large strengths with respect to the prevailing synoptic scale geostrophic wind speed, a reanalysis of the expected behavior using the full equations on a Beta plane is clearly warranted. For the present problem of Arctic LLJ's, the f plane is fully sufficient. Any observed anomalies compared to theory do not depend on the Cartesian coordinate system representation of the Coriolis forces acting. Finally, the proper representation of LLJ's in the Martian atmosphere may also need reconsideration as well due to the very small planetary radius compared with that of the Earth (see for example, Savijarvi, 1993, Joshi et. al., 1997, etc.).

. Decomposing the wind components in general into their geostrophic and ageostrophic parts, we find that the latter equations describe an inertial oscillation of the ageostrophic part of the total wind vector (if geostrophic wind speeds do not change with time) such that a clockwise rotation occurs in the N. Hemisphere (and counterclockwise in the S. Hemisphere) after "sunset". This oscillation is ideally described by a circular rotation centered about the tip of the geostrophic wind vector at "sunset" whose amplitude is the constant length of the instantaneous ageostrophic wind vector at any time during the night (a time period where z/L > 0). Observed LLJ's hodographs are rarely circular, but are instead slightly elliptical in shape, due most likely to slight frictional influences not accounted for in our standard LLJ models. During the "night" the ageostrophic wind vector maintains a constant amplitude, but turns in such a way so that the flow proceeds across the isobars oscillating first from high towards lower pressure then and back from lower towards higher pressure. At very high latitudes the LLJ process, if all else remains the same, can execute more than one low-level jet peak in a single "night" due to the shortness of the inertial oscillation period ($\equiv$ 12 hrs at the poles) compared to the length of the night (z/L > 0). This process cannot proceed however without the simultaneous thermal effects that are evident due to strong radiative or advective cooling and nocturnal inversion formation and subsequent lifting through the "night" over flat terrain under initial conditions of light winds and clear skies. This is the classical diurnal release of surface friction effect first discussed in detail in Blackadar (1957). The connection between such low-level jet formation and subsequent breakdown and the intermittent bursting phenomena analyzed in Thorpe and Guymer (1977) as well as in ReVelle (1993) and more recently in Van der Wiel et al. (2002a, 20902b, 2002c) is very intriguing and should be further investigated using wave and weakly nonlinear instability analyses. Similarly, the ageostrophic wind vector can be decomposed into its inertial and isallobaric parts, with the former component comprising effects due to frictional influences, nonlinear advective effects, etc. and the latter component which involves temporal changes.

2.1.3 Low Level Jet Wavelengths

Using the f plane approximation , it is possible to produce an expression for the wavelength of the LLJ in the form (Fleagle and Businger, 1980), namely:

$$\Lambda_{LLJ} = 2\pi\, U_g / f \qquad (7a)$$

The corresponding Rossby number of the flow, Ro, ($\equiv U/\{f_o \cdot L\}$) can be written for $U_{max} = 2 \cdot U_g$ in the form:

$Ro = 1/\pi \sim 0.32$ with $L = \Lambda_{LLJ}$ (7b)

Thus, we have shown that even the strongest LLJ's are close to satisfying hydrostatic and quasi-geostrophic theory simultaneously (Holton, 1992).

As shown below, for reasonable f and total U_g values, the Λ_{LLJ} ranges from 100-200 km at very high latitudes for typical Arctic summertime LLJ's ($1 < U_g < 5$ m/s) and increases to even larger values at lower latitudes as f decreases (and β increases).

We can also readily evaluate the ratio of this wavelength to the radius of the earth, r_e, assuming $f(y) = 2\Omega \cdot \sin\phi$. Choosing $\Lambda/r_e \leq 0.10$ for the limiting f plane approximation, we have computed the following table for the latitude, ϕ, from 30-75 deg:

Table 1. Λ_{LLJ}/r_e: f plane approximation limits

U_g: m/s	ϕ=30 °	ϕ=45 °	ϕ=60°	ϕ=75 °	Λ_{LLJ}: km
1.25	0.0175	0.0125	0.01	0.09125	618-55.5
2.50	0.035	0.025	0.02	0.01825	1236-111.5
5.0	0.07	0.05	0.04	0.0375	2472-223
10.0	0.14	0.10	0.08	0.07	4943-446

Thus, as U_g increases, the latitude for which an f plane is adequate, moves to progressively higher values. This conclusion is very similar to the conclusion we found earlier using a partial scale analysis of the full set of invisicid equations for the LLJ on a Beta plane versus those on an f plane. In addition, all wavelengths, except those at very low latitudes or at very large U_g, are within the mesoscale meteorological region, with $\lambda_{LLJ} <$ ~1000 km.

The value of ϕ, where $\Lambda_{LLJ}/r_e = 0.10$ can be very accurately described by a power law curve-fit:

ϕ (°) = $3.9282 \cdot U_g^{1.0763}$ (m/s) with $r^2 = 0.9947$ (8a)

Alternatively, given ϕ, we can find the largest U_g, that can be used for LLJ's on an f plane:

U_g (m/s) = $0.28469 \cdot \phi^{0.92415}$(°) with $r^2 = 0.9947$ (8b)

Thus, southward of 22.2 deg, the f plane approximation begins to loose its applicability for U_g = 5 m/s. For U_g = 15 m/s, the corresponding latitude of f plane validity is only northward of 72.4 deg. These are not precise latitude cut-off limits, but only reflect the increasingly poor ability of an f plane model to capture the essential physics of LLJ's as ϕ decreases. As ϕ decreases the inertial period greatly increases however, so that these limits may not be critically important to LLJ dynamics. Using the definition of the "nighttime" period in this paper, i.e., $z/L > 0$, these criterion can take on importance for low latitude descriptions of LLJ's if ϕ is not too small.

These equations loose their validity at large U_g as does the LLJ theory in general. Without light winds at "sunset", the formation and lifting of the nocturnal inversion and the subsequent frictional decoupling barrier it provides, i.e., the diurnal release of surface friction hypothesis of Blackadar, cannot proceed.

2.2 Low-level Jet Forcing Mechanisms:

There are numerous mechanisms that have been proposed for the production of LLJ's. These include (Stull, 1988, Sorbjan, 1989):

1. Isallobaric wind effects (Holton, 1992): $\partial U_g/\partial t$, i.e., nonsteady geostrophic winds
2. Baroclinicity over sloped terrain
3. Synoptic-scale baroclinicity effects
4. Thermal mechanisms on heated or cooled surfaces: Ice breezes, etc. and other effects over sloped terrain and across water-land boundaries, etc.
5. Inertial oscillations of the ageostrophic wind
6. Nonlinear advection term effects
7. Other mechanisms or combinations of the above forcing mechansims

Numerous analyses have been done to examine these factors over continental as well as coastal surfaces for $z/L > 0$ (Doyle and Warner, 1993; Arritt et. al., 1997; Parish, 2000; Anderson and Arritt, 2001; Anderson et. al., 2001, Pomeroy and Parish, 2001, etc.). Comparatively few studies have been performed for open ocean situations as considered here (Smedman et. al, 1993; Bergstrom and Smedman, 1995; Andreas et. al., 1995; ReVelle et. al., 1997; Andreas et. al., 2000; Nilsson and ReVelle, 2003- to be submitted).

Although we have considered some of these mechanisms in our LLJ modeling, the fifth mechanism above has consistently provided the best fit to observations with only one significant discrepancy, i.e., the under-prediction of the maximum LLJ strength. We have found that this deficiency is caused by our lack of ability to model the turbulent diffusivity. With an enhanced Rayleigh friction parameter as proposed below, we have found that the maximum LLJ strength prediction is greatly improved with all other parameters held constant.

3. PLANETARY BOUNDARY LAYERS: SIMPLE PREDICTIONS AND OBSERVATIONS

3.1 Simplified Predictions of ABL Parameters as a function of z/L

3.1.1 Friction velocity, u_* :

We have utilized the expression of Thorpe and Guymer (1977) for u_*, written in terms of the 10 m drag coefficient, C_D (as a function of the aerodynamic roughness length, z_o) that has been allowed to vary with z/L, for conditions not far from neutral stability:

$$u_* = 0.94 \cdot U_g^{0.80} \cdot C_D(z = 10m, f(z_o, z/L))^{0.50} \quad (9)$$

where

$$C_D = k^2/(\ln(10.0/z_o) - \psi_m(z/L))^2$$

k = Von Karman's constant (assumed = 0.40)

$\psi_m(z/L)$ = Stability correction function for turbulent momentum transfer in the surface layer

For z/L > 0 (stable):

$$\psi_m(z/L) = -(1/Ri_c) \cdot z/L \quad (10)$$

Ri_c = Critical gradient Richardson number
($Ri_c \equiv 1.0$ has been used in our analysis- see below)

This equation, which is semi-empirical, has normally been written (Stull, 1988; Sorbjan, 1989) in the form:

$$z/L = -4.7 \cdot z/L \quad (11a)$$

where

$$Ri_c = 1/4.7 \cong 0.21 \quad (11b)$$

if z/L < 0 (unstable):

$$\psi_m(z/L) = 2 \cdot \ln\{(1+x)/2\} + \ln\{(1+x^2)/2\} - 2 \cdot \tan^{-1}(x) + \pi/2 \quad (12)$$

$$x = (1 - 15 \cdot z/L)^{0.25} \quad (13)$$

3.1.2 Eddy viscosity: Prandtl's mixing length

Following Malcher and Krauss (1983), we have matched the turbulent stress between the Prandtl layer and the Ekman layer aloft. This very useful form of the eddy viscosity can be written in the form:

$$K_m = k \cdot u_* h_j \quad (14)$$

where

h_j = Altitude of the LLJ (assumed to be the top of the "nocturnal" inversion layer)

K_m = Eddy viscosity (for removal of momentum gradients in the fluid)

The very old concept of eddy viscosity (proposed for turbulent flows analogous to the role played by molecular viscosity for laminar flows) has been recently superseded in most convective boundary layer modeling by DNS (direct numerical simulation) and by LES (large eddy simulation). However, it has also been recently recognized with modern turbulence methods (through analyses by the method of multiple scales) that the eddy viscosity is still a fundamental as well as a very useful way to model turbulence with the following caveats (Frisch, 1996):

i) Two distinct scale separations must exist for the problem for eddy viscosity to be meaningful.
ii) Eddy viscosity need not be > 0 as had long been recognized by Lorenz. When it is < 0 it can lead in two-dimensions to large scale fluid instabilities.
iii) When the basic state flow problem being analyzed is not isotropic, the proper eddy viscosities are components of a fourth order tensor.
iv) When the molecular viscosity (a fundamental fluid property only dependent upon its temperature) ceases its influence on the flow and turbulence becomes dominant, both the form and importance of the nonlinear advection terms can be modified.

In order to provide a framework for future LLJ analysis and modeling efforts, we have tabulated the most significant spatial and temporal scales associated with the simplest LLJ definition (over "flat" terrain, constant geostrophic wind, f plane approximation, etc.).

Table 2. LLJ's: Scales and times of motion

Scales & times of motion	Parameter
Vertical scales: L_z	z_o: Roughness elements
	$2\pi/\lambda_z$: Turbulent diffusivity
	h_n: Inversion depth
	h_{BL} : Boundary layer depth
	z/L: Stability- Dynamical processes
	$2\pi/\lambda_g$: Wavelengths of gravity waves
Horizontal scales: L_x	LLJ: Λ_{LLJ} wavelength Mesoscale length scales
	$2\pi/\lambda_x$: Turbulent diffusivity
	Anticyclone x length scale
	$2\pi/\lambda_g$: Wavelengths of gravity waves
Time scales: τ	Inertial period: $2\pi/f$
	τ_g: Gravity wave period(s)
	Time period of z/L > 0
	Time period of z/L < 0

Clearly the multiply separated scale criterion is met for our definition of the LLJ, since in the horizontal, the scale size of an anticyclonic system is larger than that of the LLJ wavelength, which is much larger than the horizontal scale of the turbulent diffusivity of the small scale eddies that develop for z/L > 0 (stability). This does not mean that we have yet calculated the proper eddy viscosity values, only that their relevance to the problem is beyond dispute. For z/L > 0, we have also added atmospheric gravity wave properties into the above list, even though we have not formally incorporated their expected dynamical effect into the modeling (see for example Poulos et. al., 2002).

3.1.3 The turbulent Ekman number

In addition, to the above ABL parameters there are also very relevant timescales that can be inferred from the simple set of momentum equations given earlier. In addition to the inertial period, τ_i, ($\equiv 2\pi/f_o$ for the f plane approximation), there are also viscous, frictional timescales whose values depend critically on how the turbulent frictional dissipation terms are modeled. It can readily be shown that the ratio of the inertial period to the relevant frictional timescale, τ_f, is proportional to the turbulent Ekman number, Ek, of the flow, which can be written in the form:

$$\tau_i/\tau_f = 2\pi \cdot Ek \qquad (15)$$

where

$Ek \equiv (1/\rho)\cdot\partial\tau/\partial z/(f_o u)$
Ek = {Viscous force/mass}/{Coriolis force/mass}
$Ek = v_{od}/u_{od}$
τ = Surface turbulent stress in a specific direction

Thus, Ek is the ratio at "sunset" of the v component of the wind to the u component (at the end of the day, i.e., the late afternoon or when z/L > 0). These are the standard set of ABL wind components relative to the prevailing surface layer wind speed and direction and not with respect to the standard NWP, North positive and East positive Cartesian coordinate directions.

In the table below, we compare τ_i/τ_f evaluated for either a parameterized Rayleigh friction stress, τ, based on a linear proportionality between the turbulent stress and the ABL wind speed, designated as **(R)**, below in Table 3:

$$\tau = \rho C_D \cdot \{U_g/2\} u \qquad (16a)$$

$$\tau_f = h_i/k_s = 2h_i/(C_D \cdot U_g) \qquad (16b)$$

such that:

$$\tau_i/\tau_f = \pi C_D \cdot U_g/(h_i \cdot f_o) \qquad (17)$$

If instead we utilize a first order closure scheme designated as **(K_m)**, in Table 3 below, as proposed above in equation (14):

$$\tau = \rho K_m \cdot \partial U/\partial z \qquad (18a)$$

$$\tau_f = h_i^2/K_m \qquad (18b)$$

such that:

$$\tau_i/\tau_f = 2\pi \cdot K_m/(h_i^2 \cdot f_o) \qquad (19)$$

where

h_j = Boundary layer inversion height at "sunset"
$f_o = 1.4584 \cdot 10^{-4}$ s^{-1} ($\equiv$ value at the pole) = α (*)

These timescale ratios are evaluated in Table 3 below.

Table 3. Slab model timescale ratio: z/L= 1.0

f_o: s^{-1}	h_j: m (**)	z_o: m	U_g: m/s	τ_i/τ_f: (R)	τ_i/τ_f: (K_m)
α (*)	200.0	10^{-3}	1.0	0.165	3.173
α (*)	200.0	10^{-3}	2.0	0.331	5.525
α (*)	200.0	10^{-3}	3.0	0.496	7.641
α (*)	200.0	10^{-3}	4.0	0.661	9.619
α (*)	200.0	10^{-2}	1.0	0.276	4.097
α (*)	200.0	10^{-2}	2.0	0.551	7.133
α (*)	200.0	10^{-2}	3.0	0.827	9.867
α (*)	200.0	10^{-2}	4.0	1.102	12.42

(**) Typical AOE-96 observations have "sunset" mixing layer depths of $100 \le h_d \le 300$ m.

Rearranging equation (31) and solving for the turbulent Ekman number, we have the expression:

$$Ek = (1/2\pi)\cdot\{\tau_i/\tau_f\} \qquad (20)$$

$$\therefore\ Ek = (1/f_o)\cdot C_D \cdot U_g/(2\cdot h_i) \qquad (21a)$$

for a standard Rayleigh friction turbulence model and:

$$\therefore\ Ek = (1/f_o)\cdot K_m/h_j^2 \qquad (21b)$$

for a first order closure, K theory approach to modeling the turbulent stresses acting.

Results for these three variables (u_*, K, and Ek) for the case of z/L = 0.0 are presented below in Figures 1-3.

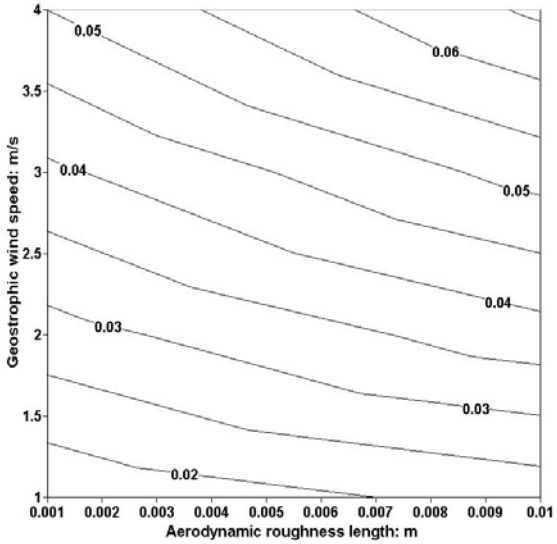

Figure 1: Friction velocity in m/s as a function of the prevailing geostrophic wind speed in m/s and of the aerodynamic roughness length in m.

Anticipating the standard conditions for case9603 in AOE-96 discussed later below, the predicted friction velocity is ~0.045 m/s with a corresponding eddy viscosity of ~2 m^2/s. Much more complicated predictions of eddy viscosity from the 1-D BLMARC model (see below) during this period correspond to K = ~0.35 m^2/s, although variable in time (for z/L = 0.0).

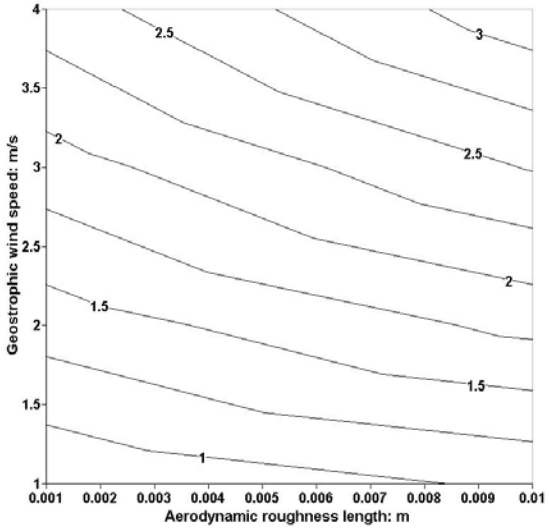

Figure 2: "Eddy" viscosity in m^2/s versus the prevailing geostrophic wind in m/s and the aerodynamic roughness length in m.

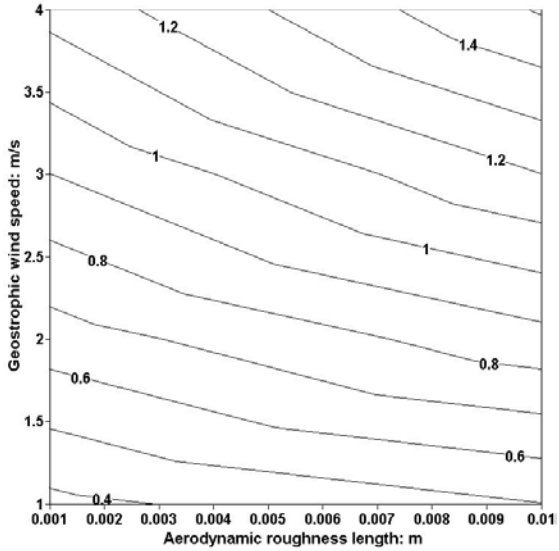

Figure 3: Dimensionless Ekman number versus the prevailing geostrophic wind speed in m/s and the aerodynamic roughness length in m.

It should be noted that the Ek > 1 limit is just reached for the situation with U_g = 2.5 m/s and z_o = 0.01 m.

3.2 Enhanced Thorpe and Guymer Model

Thorpe and Guymer (1977) produced an analytic model (TG77) of the atmospheric, nocturnal low-level jet using the mechanism proposed by Blackadar of the diurnal release of surface friction that produces an inertial oscillation of the ageostrophic wind component. It is the simplicity of this model that we are appealing to here because the full complexity of the general case, for example including synoptic-scale baroclinicity, is not completely understood either (see for example, ReVelle and Liu, 1992).

Anticipating our results below, we have now been able to significantly correct the one remaining deficiency in the TG77 model, namely the fact that the maximum LLJ strength was not predicted to be sufficiently strong as compared with observations. The other significant advantage of using this model for the case of the Arctic LLJ's is that many of the other mechanisms discussed earlier are probably not applicable so that the essential physics has been captured for the inviscid part of the model, i.e., the LLJ. The predicted behavior of the viscous "daytime" and "nighttime" winds still has not been fully corrected by our enhanced model, but this was not really expected, since a multi-level model, such as BLMARC (see below), is probably needed to more fully capture the correct behavior of these flow coupled turbulent, dissipative solutions. The simplicity of TG77 is also

readily amenable to the performance of a sensitivity analysis as we will discuss later below.

These model solutions can be represented by the following set of equations of day (mixed layer frictional wind) and by night (frictional wind component below the nocturnal inversion and finally by the frictionless LLJ above the nocturnal inversion):

$$|V_{df}/U_g| = f^2U_g/A_d + fU_gk_s/(h_dA_d)\cdot i + C_{df}^{*}\exp[-(if + k_s/h_d)t] \quad (22)$$

$$|V_{nj}/U_g| = U_g + C_{nj}^{*}\exp[-i\cdot ft] \quad (23)$$

$$|V_{nf}/U_g| = f^2U_g/A_n + fU_gk_s/(h_nA_n)\cdot i + C_{nf}^{*}\exp[-(if + k_s/h_n)t] \quad (24)$$

where

V_{df} = Total "Day" wind speed at all levels for the mixed layer from "sunrise" and sunset"
V_{nj} = Total "Night" wind speed of the low-level jet above the inversion level
V_{nf} = Total "Night" frictionally damped wind below the inversion level
U_g = Prevailing synoptic-scale geostrophic wind, i.e., the vector sum of the u (East) and v (North) components of the geostrophic wind
$A_d = (k_s/h_d)^2+f^2$
$A_n = (k_s/h_n)^2+f^2$
k_s = $C_D\{U_g/2\}$; Standard Rayleigh friction parameter
$k_s' = K_m/h_j$; Enhanced Rayleigh friction parameter with 1st order closure stress matching
C_D = 10 m drag coefficient as a function (z_o, z/L)
h_d = Height of the daytime mixed layer
h_n = Height of the nocturnal inversion layer
t = time (with t = 0 corresponding to "sunset")

$C_{df}^{*} = C_{df} + C_{df}'i$; "Day-time" mixed layer
$C_{nf}^{*} = C_{nf} + C_{nf}'i$; "Nocturnal" inversion layer
$C_{nj}^{*} = C_{nj} + C_{nj}'i$; "Nocturnal" LLJ
$i = \sqrt{-1}$

The terms in C_i^{*} are complex initial conditions that must be solved subject to the prescribed boundary conditions, namely:

"Sunset", i.e., t = 0 in the nocturnal equations:

$$|V_{df}| = |V_{nj}| = |V_{nf}| \quad (25)$$

or equivalently in terms of components:

$$u_d = u_{nf};\ u_d = u_{nj};\ v_d = v_{nf};\ v_d = v_{nj} \quad (26)$$

"Sunrise", i.e., $t \rightarrow \infty$ in the daytime solutions:

$$|V_{df}| = \{h_n/h_d\}\cdot|V_{nf}| + \{1 - h_n/h_d\}\cdot|V_{nj}| \quad (27)$$

Solving for the various C_i^{*}, we have the resulting solutions:

"Daytime", frictionally damped mixed layer:
$t_L \equiv$ length of the "night", i.e., time when z/L > 0

$$C_{df} = f^2U_g\{A_dh_n - A_nh_d\}/\{A_d\cdot A_n\cdot h_d\} + \{1-(h_n/h_d)\}\cdot\{U_g + C_{nj}\cdot cosft_L + C_{nj}'\cdot sinft_L\} \quad (28a)$$

$$C_{df}' = fk_sU_g\{(A_d - A_n)/(A_d\cdot A_n\cdot h_d) + \{1-(h_n/h_d)\}\cdot\{C_{nj}'\cdot cosft_L - C_{nj}\cdot sinft_L\} \quad (28b)$$

"Nocturnal", Low-level jet layer:

$$C_{nj} = u_o - U_g \quad (29a)$$
$$C_{nj}' = v_o \quad (29b)$$

"Nocturnal", frictionally damped layer:

$$C_{nf} = f^2U_g\{A_n - A_d\}/\{A_nA_d\} \quad (30a)$$
$$C_{nf}' = fk_sU_g\{(A_nh_n - A_dh_d)/(\{A_nh_n\}\{A_dh_d\})\} \quad (30b)$$

By substituting the complex initial conditions into the original equations for the wind solutions for "day", "night" and "night-jet" components, we can then equate real and imaginary parts and solve for the individual {u,v} wind components for the three solutions in the form:

"Daytime" frictionally damped mixed layer:

$$u_{df} = f^2U_g/A_d + C_{df}\cdot\exp[-\{k_s/h_d\}t]\cdot cosft + C_{df}'\cdot\exp[-\{k_s/h_d\}t]\cdot sinft \quad (31a)$$

$$v_{df} = fU_g\{k_s/h_d\}/A_d - C_{df}\cdot\exp[-\{k_s/h_d\}t]\cdot sinft + C_{df}'\cdot\exp[-\{k_s/h_d\}t]\cdot cosft \quad (31b)$$

"Nocturnal", Low-level jet layer:

$$u_{nj} = U_g + (u_o - U_g)\cdot cosft + v_o\cdot sinft \quad (32a)$$

$$v_{nj} = -(u_o - U_g)\cdot sinft + v_o\cdot cosft \quad (32b)$$

where

$$u_o = u_{df}\ (t\rightarrow\infty) = f^2U_g/A_d = u_{nf}\ (t = 0) \quad (33a)$$
$$v_o = v_{df}\ (t\rightarrow\infty) = fk_sU_g/(A_d\cdot h_d) = v_{nf}\ (t = 0) \quad (33b)$$

"Nocturnal", frictionally damped layer:

$$u_{nf} = f^2 U_g / A_n + C_{nf} \cdot \exp[-\{k_s/h_n\}t] \cdot \cos ft + C_{nf}' \cdot \exp[-\{k_s/h_n\}t] \cdot \sin ft \quad (34a)$$

$$v_{nf} = f U_g \{k_s/h_n\}/A_n - C_{nf} \cdot \exp[-\{k_s/h_n\}t] \cdot \sin ft + C_{nf}' \cdot \exp[-\{k_s/h_n\}t] \cdot \cos ft \quad (34b)$$

Solutions of these equations will produce strong LLJ's if $\tau_l/\tau_f > 2\pi$ (so that processes with the short timescales will dominate) and a large geostrophic departure will be evident at "sunset". In the opposite case, since $\tau_l/\tau_f << 2\pi$, LLJ's cannot be established.

Unfortunately, only the K_m method (whose ratios are 10-20 times > the standard Rayleigh friction approach) can give $\tau_l/\tau_f > 2\pi$ for these parameters as was seen in Table 3 earlier. In this paper the expression for k_s' originates by equating these two frictional timescales and solving for K_m in terms of k_s.

Using the AOE-96 observational parameters for case 9603, we have established the following reference numerical values for the key parameters also utilized in the sensitivity study that will be discussed later (all cases were evaluated with the length of day = 2 hrs and with $\phi = 90°$):

Reference numerical values (from AOE-96):

z_o = 0.01 m
U_g = 2.5 m/s
h_d = 500.0 m
h_n = 100.0 m
z/L = 0.0

The z_o listed above is a maximum for the conditions encountered. More realistic values are as much as 10 times lower. Fortunately, the predicted LLJ response will not change very much with our enhanced model result where the maximum LLJ wind speed compared to U_g only decreases to 1.40.

We now plot the Thorpe and Guymer (1977) normalized model solutions (with respect to the prevailing synoptic-scale geostrophic wind speed) with U_g available from AOE-96 data) for two different Rayleigh friction values, with t = 0 indicating "sunset", namely:

i) Frictionally damped winds and the inviscid LLJ winds using the standard Rayleigh friction in TG77.

ii) Frictionally damped winds and the inviscid LLJ winds using the enhanced Rayleigh friction predicted in this paper.

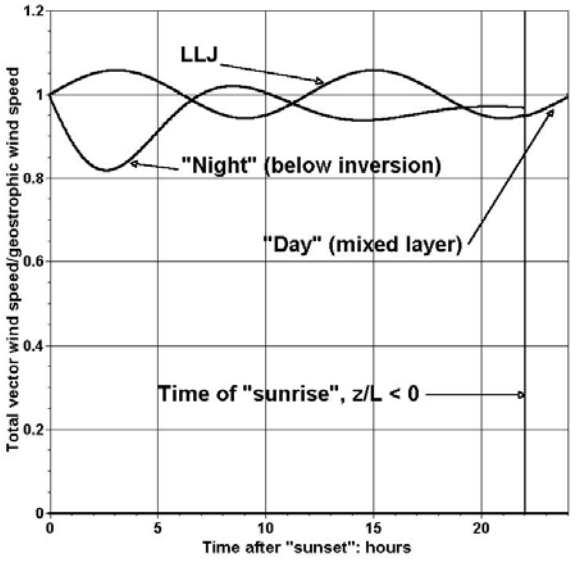

Figure 4: Normalized, total vector "day", "night" and LLJ winds: Standard TG77 results.

The enhanced Rayleigh friction effect on the LLJ in Figure 5 is equivalent to increasing z_o by ~100 times in Figure 4. Note also however that the "nighttime" winds for the enhanced prediction below the inversion are not only far lower early in the "night' than for the TG77 case, but are also nearly constant. In addition, the LLJ is sufficiently weak for the standard TG77 that the predicted frictional winds below the inversion are comparable to the LLJ during most of the night, which is clearly unrealistic compared with our observations.

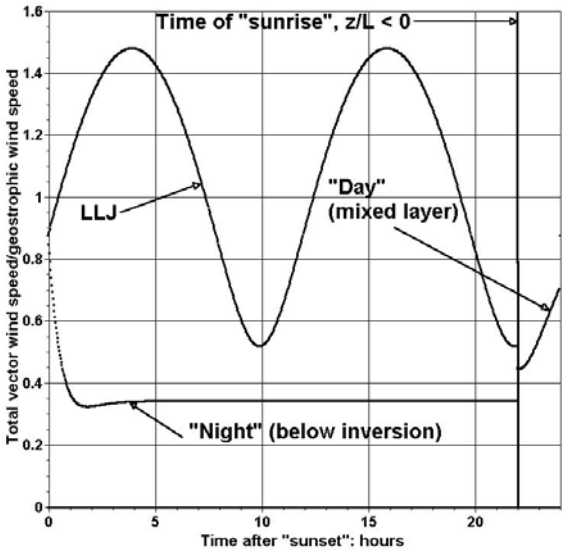

Figure 5: Normalized, total vector "day", "night" and LLJ winds: Enhanced Rayleigh friction results developed in this paper.

The enhanced results have increased the LLJ winds dramatically compared to the standard TG77 results.

The predicted hodograph representations through time of the "nocturnal" winds for which z/L > 0 in Figures 4 and 5 are also given below in Figure 6.

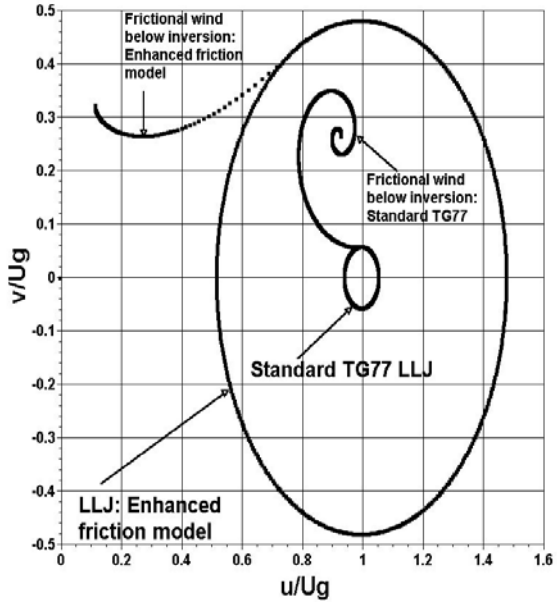

Figure 6: Hodograph depiction of the winds for which z/L > 0 from the results n Figures 4 and 5.

We have also plotted below the contoured ratio of the enhanced Rayleigh friction parameter to that originally used in TG77 as a function of U_g and of z_o.

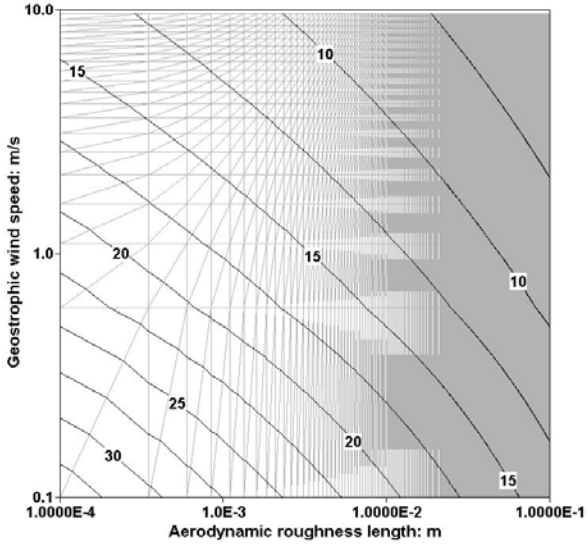

Figure 7: Contoured values of the ratio of the enhanced Rayleigh friction term in this paper compared to the standard TG77 (for z/L = 0.0).

The expression for this ratio can be simplified to the following explicit form:

$$k_s'/k_s = \{K_m/h_j\}/(C_D \cdot U_g/2) \quad (35a)$$

or:

$$k_s'/k_s = 0.752 \cdot U_g^{-0.20}/C_D(z = 10.0, z_o, z/L)^{1/2} \quad (35b)$$

In Figure 7, it is readily observed that the ratio of these terms. I.e. the enhanced estimate of the Rayleigh friction parameter, K_m/h_j, compared to the standard value used in Thorpe and Guymer (1977), $C_D \cdot (U_g/2)$, becomes quite large at very small geostrophic wind speeds and aerodynamic roughness lengths. The limiting value for z/L = 0.0 is ~55 and approaches only ~2.4 as these two parameters approach their realistic upper limits in the atmospheric boundary layer (for example, for U_g = 20 m/s with z_o = 1.0 m, respectively). The result of this enhanced ratio is that significantly larger LLJ's are possible over a lower boundary (either continental or oceanic or ice, etc.) with quite small aerodynamic roughness and small U_g, whereas over a very rough lower boundary with strong prevailing U_g, where LLJ's are already predicted to be quite strong and only small increases in LLJ wind speed are predicted. This ratio is predicted to be even somewhat greater at larger positive z/L values, but again almost entirely over quite smooth surfaces for small values of U_g.

Finally, the Thorpe and Guymer (1977) theory can also predict the cross-isobar flow angles of the winds that are directly controlled by turbulent frictional influences, and these can be written for the "day-time" mixed layer and for the "night-time" (below the inversion level) winds in the form as can also readily be observed in Figure 6:

$$\alpha_d = \tan^{-1}(v_d/u_d) \quad (36a)$$

$$\alpha_n = \tan^{-1}(v_n/u_n) \quad (36b)$$

Typical predicted maximum "day-time" cross-isobar flow angles are predicted to range from 10°-45°, whereas typical maximum "night-time" angles range from 20°-70 ° due to the generally larger frictional influence acting on the flow, depending on z/L, etc. The predicted temporal cross-isobar flow angles for the conditions in Figure 5 are given below in Figure 8. It should be noted in Figure 8 that after about 3 hours past "sunset", the predicted lower level, cross-isobar flow angle of the winds is essentially constant, whereas from the hodograph for the standard TG77, it is clear that this is not predicted to occur. In this standard TG77 case a weaker, frictionally damped wind oscillation continues to be predicted throughout the "night".

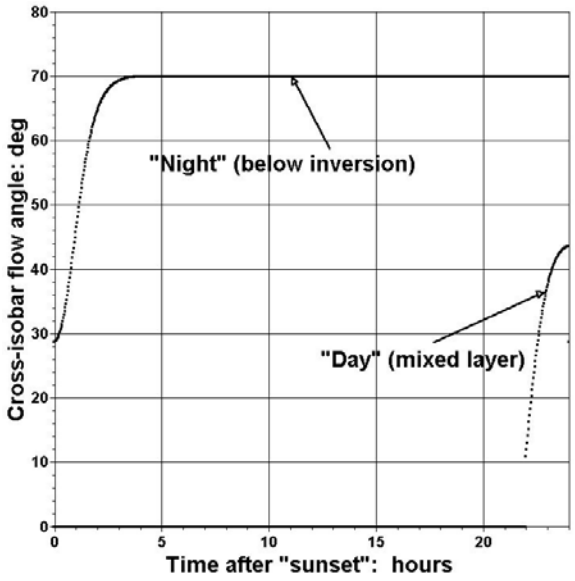

Figure 8: Predicted cross-isobar flow angle (deg) for the "night" (below the inversion layer) and for the "day" (mixed layer) for the enhanced Rayleigh friction conditions indicated in Figure 5.

We are continuing to investigate whether or not LLJ's of considerable strength compared to the geostrophic wind can be maintained over quite smooth surfaces with light geostrophic winds as the surface layer stability, as measured by z/L, becomes large and > 0. It is highly probable in our opinion, however that eventually a limiting constraint will be imposed on the system, so that sustained further growth of LLJ maximum winds will be improbable.

3.3 Thorpe and Guymer Model: LLJ Senstivity Study

We have taken advantage of the analytic simplicity of the Thorpe and Guymer model to perform a sensitivity study of all of the LLJ parameters on the resulting maximum LLJ wind strength. To be sure some very important physics has been left out of the problem in order to gain the simplicity necessary to get an analytic solution, but within the framework of the retained physics, we can rapidly get a clear indication of what parameter is acting to either enhance or reduce the strength of the LLJ. The key parameters that have been examined include the aerodynamic roughness length, the geostrophic wind, the heights of the "daytime" mixed layer and of the "nighttime" inversion layer, the drag coefficient as a function of z/L, the frictional parameterization term (Rayleigh friction parameter or K theory enhancement to the Rayleigh friction term, etc.). ReVelle, Logsdon and Liu (1990) carried out a similar study using a simpler system of equations, but also included the possibility of square law drag in the surface layer as well. They also determined that the turbulent Ek was a significant factor in predicting the LLJ maximum wind strength. It should be noted that their predicted dependence of Ek on the maximum LLJ wind speed was linear, i.e, for an Ek = 1.0, the maximum LLJ winds attained a value that was twice as strong as the value determined for a situation in which Ek = 0.50 at "sunset".

The height of the nocturnal inversion was not varied during the sensitivity analysis since it was not found at the onset not to produce a significant effect on the maximum LLJ wind speed. As the height of the "nighttime" inversion layer decreased the strength of the frictional wind below the inversion rapidly decreased. The same behavior was found if instead we allowed the height of the inversion layer to be larger with all other parameters maintained at the ir same original value.

Anticipating our subsequent sensitivity analysis, it is clear that we should expect that the jet maximum should get stronger as the aerodynamic roughness length increases since this parameter controls the degree of frictional influence of the lower boundary on the low-level wind systems. Eddies formed near the ground have a scale size comparable to the roughness elements themselves which are larger than the aerodynamic roughness length by ~6-30 times (with the larger value appropriate over regions with smaller z_o). Effects of further pressure drag due to significant terrain features in various directions have not been incorporated into these simple descriptions of the lower boundary. Fortunately, summertime LLJ's over the high Arctic Ocean should not be significantly affected by such terrain effects.

It is also clear that the geostrophic wind should greatly influence the maximum LLJ wind since the geometry of the original Blackadar system depends critically on rotating the ageostrophic wind vector with respect to the original geostrophic wind vector, i.e., the strength of the LLJ is due to the vector addition of the ageostrophic and the geostrophic wind components though time periods when z/L > 0. Finally, since the geostrophic departure depends upon the late afternoon profile (z/L< 0 in this case) including the height of the mixed layer, the expected important dependence of the maximum LLJ wind speed on the daytime mixed layer height is consistent with what we have already determined about what controls the strength of the maximum LLJ wind speed though the Ekman layer at "sunset".

The general range of applicability of z/L should be from $-\infty < z/L < \infty$, but the empirical fitting constants, are all based on field observations over essentially "flat", terrain (with very small slopes) and are available only under a limited range of meteorological

conditions. Thus, the necessary constants are only known for fitting the stability/instability functions over a much smaller dynamic range (-10 < z/L < 2.0, Sorbjan; 1989). The stable flow limit of large positive z/L has not yet been adequately addressed yet however due to complexities arising from the presence of gravity waves, intermittent turbulence with the presence of coherent structures, etc. In addition, theoretical analyses including the very important effects of long wave radiation cooling on the Monin-Oboukhov-Lettau length for large positive z/L have not been performed. In addition, knowledge of the critical transition Richardson number(s) for transition from laminar to turbulent or from turbulent to laminar flow are also only known within certain limits partly due to the hysteresis inherent in the system and partly due to the fact that the resulting value depends on the physical processes accounted for in the theoretical derivation, i.e., "linearity" of amplitudes, etc. Theoretical analyses indicate a critical transitional gradient Richardson number ranging from $1 > Ri_c > 0.25$ whereas field and laboratory measurements range from $1 > Ri_c > 0.20$. The best value however (if a single value exists) would seem to be $Ri_c = 1.0$ (Miles, 1986, ReVelle, 1997, Cheng et. al., 2002), but additional factors such as water vapor in the air also can modify the critical transitional Ri_c value (Lalas and Einaudi, 1973). The empirical expression for the drag coefficient at the 10 m level used earlier was developed based on a $Ri_c = 0.213$ (= 1.0/4.7) even though we actually utilized $Ri_c = 1.0$. There is the additional complication that most models do not resolve the surface layer adequately enough so that the proper evaluation of a finite difference, bulk gradient Richardson number to be compared with Ri_c is not reliable as well. For the Thorpe and Guymer model this is not an issue since the Richardson number itself is not formally evaluated at multiple levels within the surface layer and it is only evaluated analytically at the LLJ level.

We have performed our sensitivity analysis by evaluating each parameter one at a time with all of the other parameters held fixed, while maintaining a fixed latitude (ϕ = 90 deg). Of the parameters evaluated, the four most important ones for maximizing the strength of the LLJ wind were the aerodynamic roughness length, the magnitude of the reference synoptic scale geostrophic wind speed, the height of the daytime mixed layer and finally the stability of the surface layer as measured by z/L. The maximum limit of twice the geostrophic wind speed was confirmed during the evaluation of these parameters as expected from the dynamical and geometrical behavior of the original Blackadar model. It was determined that the maximum possible LLJ wind speed was approached as either z_o increased or as the reference U_g increased or as h_d decreased. As the peak LLJ winds increased the corresponding frictionally damped "day" and "night" winds decreased. For the opposite tendency of z_o decreasing, U_g decreasing and h_d increasing, the LLJ maximum winds decreased and the "day" and "night" frictional winds became much stronger.

An evaluation of the effects of surface layer stability on the resulting LLJ winds produced the result that for z/L > 0, the LLJ wind maximum was progressively smaller. For z/L < 0, we found that the LLJ winds strengthened greatly, but this limit is not a physically valid one to examine, since the corresponding probability of the formation of a surface based inversion layer over "flat" terrain by long wave radiation cooling is very unlikely with z/L < 0.

Also, as we changed the closure technique from zeroth order to our enhanced Rayleigh friction parameter using first order closure matching, the speed of both the "day-time" mixed layer winds and the "night-time" winds below the inversion also increased slightly for z/L > 0 and increasing, whereas using the standard Rayleigh friction approach they actually decreased slightly (the opposite behavior occurred for z/L increasingly negative however).

A summary of the predicted sensitivities of the LLJ and of the day and night frictional winds for the key parameters, including f_o, for TG77 is provided below.

Table 4. Thorpe and Guymer model sensitivities

Boundary layer response	**LLJ wind speed**	**Day-time (mixed layer) wind**	**Night-time wind (beneath inversion layer)**
f_o (An optimum ϕ may exist for peak LLJ winds	**↑ as f_o decreases Larger Ek number**	**↓ slightly as f_o decreases**	**↓ as f_o decreases**
z_o	**↑ as z_o increases**	**↓ as z_o increases**	**↓ as z_o increases**
U_g	**↑ as U_g increases**	**↓ as U_g increases**	**↓ as U_g increases**
h_d	**↑ as h_d decreases**	**↑ slightly as h_d increases**	**Almost no effect**
h_n	**Almost no effect**	**Almost no effect**	**↓ as h_n decreases**
k_s (or k_s') for z/L ≡ 0	**↑ as k_s increases**	**↓ as k_s increases**	**↓ as k_s increases**
z/L	**↓ slightly for z/L larger (and > 0)**	**↑ slightly for z/L larger (and > 0)**	**↑ slightly for z/L larger (and > 0)**

This predicted increase in the maximum jet wind speed has been found to produce a much better agreement with observations, although it is still an underestimate compared to the observed values. This substantially predicted improvement in LLJ strength is significant because we have not had to appeal to the either the nonlinear advection terms (not currently included in the model) or to other types of forcing to get better agreement with the existing observations. Of all of the possible types of advective terms that could be successfully incorporated into the LLJ modeling process, it is the vertical advection terms that are easiest to include accurately if a reliable estimate of the vertical motion field can be provided (using a mesoscale numerical model for example). We are still left with the problem of providing a reliable estimate of the vertical shear of the wind field itself and of the geostrophic wind (in order to incorporate baroclinicity) in particular which is not easy however.

As noted earlier the predicted strength of the LLJ can be captured by a single similarity variable, the turbulent Ekman number (that is now corrected for both stability and for the manner in which the frictional drag is accounted for in the model, using either the standard TG77 or our enhanced approach), The peak LLJ magnitude has been found to be proportional to the degree of geostrophic departure at "sunset", i.e., the time at which the surface boundary layer transits to a condition with $z/L > 0$ (stability). Finally, as expected, the period of the LLJ inertial oscillation was exactly 12 hrs at the pole as is clearly evident in the behavior of the LLJ total wind vector.

3.4 The BLMARC Model

In preparation for the AOE-96 expedition, we developed an expanded and quite flexible 1-D computer code based on the successful work of ReVelle (1993) and of ReVelle and Coulter (1994; 1995) on modeling of boundary layer "bursting", i.e. the transition to laminar flow from a prior turbulent state and vice versa. This new code, **BLMARC** (Boundary Layer, Mixing, Aerosols, Radiation and Clouds), explicitly includes the physical and chemical effects due to the presence of clouds, aerosols and the associated air chemistry. The aerosol model has been developed by Kulmala et. al. (1991, 1995). Briefly the model utilizes a 4^{th} order Runge-Kutta numerical finite difference method to calculate the temperature and winds in very small, linear vertical layer increments using a surface layer energy balance scheme with a force restore treatment of the lower boundary, combined with a Monin-Oboukhov surface layer physics calculation beneath an Ekman layer using eddy viscosities calculated using first order closure with a finite difference bulk gradient Richardson number evaluation compared to a critical Richardson number utilized to compute the surface layer stability at all times. Long wave radiation at all model levels including the ground interface is incorporated using an approximate scheme based on the amount of water vapor and carbon dioxide present in the model. The scheme must be properly initialized using rawinsonde data as well as surface properties (soil type and conductivity, temperature versus depth, etc.). Water vapor and its unsaturated and saturated thermodynamic effects have been incorporated using the moisture availability parameter. Geostrophic winds (barotropic, baroclinic, constant or variable with time) are input to the model on the basis of our evaluation of these parameters from available mesoscale analyses.

From the AOE-96 expedition, we initially chose two time periods to model with **BLMARC**:

1. Case9603: July 27,1996
(83.77 N, 66.14 E): Very Stable PBL

2. Case9604: July 29, 1996
(85.55 N, 72.22 E): Extremely Stable PBL.

All data have been used wherever possible to both initialize the model runs and also to help test/validate the model outputs. Both 24 hour periods were indicative of barotropic and highly stable conditions with periods of clear skies and light winds, etc., prevailing for two days prior to the initialization period.

Case 9603 was a time period that exhibited a great detail of very interesting boundary layer physics. Preliminary runs using **BLMARC** demonstrated quite good agreement between measurements of temperature and winds and the model predictions over a 12 hr time period. Temperature predictions were excellent compared with the measurements, but even wind speeds and directions were reasonably well predicted. This case will be discussed in great detail in the forthcoming paper of Nilsson and ReVelle (see below) including the relevant synoptic situation and the state of the Arctic pack ice, etc.

The second period chosen exhibited periods of oscillations of temperature and winds and of aerosol concentrations observed during helicopter flights. During at least part of this period the aerosol concentration oscillations were correlated with those of the temperature and winds in the lowest layers. The latter case was subsequently investigated using a different approach, when it was ultimately realized that the Icebreaker Oden had inadvertently interfered aerodynamically with the wind speed and wind direction measurements (Bigg et. al., 2001).

Although full details will be provided elsewhere (Nilsson and ReVelle, 2003, to be submitted), we have completely analyzed one month of wind observations from the AOE-96 expedition and have performed FTT spectral analyses on these data.

Although several longer timescales are also evident, such as those associated with synoptic and diurnal influences specifically, as expected, as well as spectral maxima at shorter timescales from 1-5 hours, a dominant spectral peak was also found at a timescale nearly equal to that of the inertial period at these very high latitudes, i.e., 12 hours. This fact is very significant and supports our interpretation of LLJ's in terms of an inertial oscillation mechanism.

4. SUMMARY AND CONCLUSIONS

4.1 Alternative LLJ Production Mechanisms

Although we have emphasized the inertial oscillation theory first developed by Blackadar (1957) over nocturnal (stable) continental locations for conditions of relatively clear skies and light winds, other explanations can also be possible since we still cannot fully explain the strength of the LLJ as compared with observations. As is well known, the Blackadar theory, in the absence of slope effects or of baroclinicity or of nonlinear advection effects, etc., predicts the maximum magnitude of the LLJ strength to be exactly twice the magnitude of the prevailing synoptic scale geostrophic wind speed. To be sure this latter quantity is hard to determine accurately, especially when the prevailing pressure gradient is very weak, but this hardly seems to be the dominant explanation for the observed speed discrepancy. Most probably, in addition to this fundamental uncertainty in the reference geostrophic wind speed, other small and accumulating flow processes are likely to be at work which modify the simplest theories we have used for an f plane description of the LLJ phenomena. Some of the largest wind speed discrepancies have been observed for the Koorin LLJ (Brook, 1985), where the ratio of the maximum jet speed to the geostrophic speed has exceeded a factor of four. In addition to additional forcing mechanisms, the Koorin LLJ occurs at quite low latitudes in northern Australia where we have shown that the utilization of an f plane description is probably an important part of the overall modeling deficiency.

4.2 Explanations of Observed Arctic Summertime Low-level Jets

We have proposed in this paper that we can use the inertial oscillation theory of the ageostrophic wind components to explain the observed summertime LLJ's over the high latitude Arctic ocean using a modified form of the original theory of Blackadar. In this approach we have replaced the concept of the time of "sunset", i.e., where the normal period of continental nocturnal cooling occurs, with a time period over the ocean during which the atmospheric surface boundary layer is stable, i.e., $z/L > 0$. In addition, the time of "sunrise", must also be replaced with a stability change from $z/L > 0$ to one of $z/L < 0$.

In our treatment we have also allowed for an enhanced Rayleigh friction parameter that predicts substantially larger maximum LLJ wind speeds compared with the original TG77 model prediction for such smooth surfaces, i.e., over regions with quite small aerodynamic roughness lengths. This approach is fully justifiable on the basis of the large-scale separation between the typical mesoscale, low-level jet wavelength and the very small horizontal scale of the eddy viscosities of the stable, surface boundary layer. This new approach has allowed more frictional influences in regions below the LLJ in the near-surface inversion layer with resulting stronger LLJ wind maximum compared to earlier TG77 model predictions for exactly the same LLJ parameters.

In between these two time limits, the original Blackadar and Thorpe and Guymer theories are applicable depending on the duration of an inertial oscillation period as a function of latitude compared to the time that $z/L > 0$ in the spatial region that the LLJ occupies and upon the wavelength of the resulting LLJ compared to a typical horizontal spatial scale of an anticyclonic, high pressure region. In addition, there is also the question of the surface aerodynamic roughness length as a function of the prevailing wind direction and of the influence of substantial surface features in various directions upstream of the flow as well as the distribution of the summertime ice pack extent and on the changing surface boundary layer thickness, and on additional factors.

4.3 Future Work

Using data from AOE-96 and the TG77 enhanced model as well as our 1-D **BLMARC model**, we have begun a systematic effort to compare observations of the high Arctic summertime boundary layer temperatures and winds against numerical modeling results. Preliminary results for LLJ winds for case9603 is quite promising as will be reported on shortly (Nilsson and ReVelle, 2003; to be submitted).

Current work also includes model experiments with **BLMARC** on the aerosol nucleation and growth in the Arctic ABL and on cloud and fog formation.

5.0 ACKNOWLEDGMENTS

This collaborative work first began in the fall of 1995 during the first author's visit to the Meteorological Institute of Stockholm University (MISU) to work with E.D. Nilsson when **BLMARC** was first conceived. Numerous supported visits over the past 8 years, for which the first author is very grateful, have proven to be very productive. The present work grew out of the

first author's visit to MISU in September of 2002 and from course materials on the low-level jet that he has been developing over the past decade.

6.0 REFERENCES

Anderson, C.J. and R.W. Arritt, 2001: Representation of summertime low-level jets in the central United States by the NCEP-NCAR reanalysis, J. Climate, 14, 234-247.

Anderson, B.T., J.O. Roads, S.-C. Chen and H.M.H. Juang, 2001: Model dynamics of summertime low-level jets over northwestern Mexico, J. Geophys. Res., 106, 3401-3413.

Andreas, E.L., K.J. Claffey and M.P. Makshtas, 1995: Low-level atmospheric jets over the western Weddell Sea, Paper 12.1, Preprint Volume of the 4th Amer. Meteor. Soc. Sympos. on Polar Meteor. and Ocean., 252-257.

Andreas, E.L., K.J. Claffey and A.P. Makshtas, 2000: Low-level atmospheric jets and inversions over the western Weddell Sea, Bound.-layer Meteor., 97, 459-486.

Anthes, R. A., 1980: Boundary layers in numerical weather prediction, Workshop on the planetary boundary layer, Editor, J.C. Wyngaard, American Meteor. Soc., Boston, Mass., 322 pp.

Arritt, R.W., T.D. Rink, M. Segal, D.P. Todey, C.A. Clark, M.J. Mitchell and K.M. Labas, 1997: The Great plains low-level jet during the warm season of 1993, Month. Weath. Rev., 125, 2176-2192.

Banta, R.M., R.K. Newsom, J.K. Lundkuist, Y.L. Pichugina, R.L. Coulter and L. Mahrt, 2002: Nocturnal low-level jet characteristics over Kansas during CASES-99, Bound.-Layer Meteor., 105, 221-252.

Bergstrom, H. and A.-S. Smedman, 1995: Stably stratified flow in a marine atmospheric surface layer, Bound.-Layer Meteor., 72, 239-265.

Bigg, E.K., C. Leck and E.D. Nilsson, 2001: Sudden changes in aerosol and gas concentrations in the central Arctic marine boundary layer: Causes and consequences, J. Geophys. Res., 106, 32167-32185.

Brook, R.R., 1985: Koorin nocturnal low-level jet, Bound.-Layer Meteor., 32, 133-154.

Blackadar, A.K., 1957: Boundary layer wind maxima and their significance for the growth of nocturnal inversions, Bull. Amer. Meteor. Soc., 38, 283-290.

Cheng, Y., V.M. Canuto and A.M. Howard, 2002: An improved model of the turbulent PBL, J. Atmos. Sci., 59, 1550-1565.

Corsmeijer, U., N. Kalthoff, O. Kolle, M. Kotzian and F. Fiedler, 1997: Ozone concentration jump in the stable nocturnal boundary layer during a LLJ-event, Atmos. Environ., 31, 1977-1989.

Doyle, J.D. and T.T. Warner, 1993: A three-dimensional numerical investigation of a Carolina coastal low-level jet during GALE IOP 2, Month. Weath. Rev., 121, 1030-1047.

Fleagle, R.G. and J.A. Businger, 1980: An Introduction to Atmospheric Physics (Second edition), Academic Press, Inc., New York, 432 pp.

Frisch, U., 1996: Turbulence, Cambridge University press, Cambridge, 296 pp.

Gill, A.E, 1982: Atmosphere-Ocean Dynamics, Academic Press, Inc., Orlando, 662 pp.

Holton, J. R. 1992: An Introduction to Dynamic Meteorology (Third edition), Academic Press, Inc., New York, 511 pp.

Joshi, M.M., R.M. Haberle, J.R. Barnes, J.R. Murphy and J. Schaeffer, 1997: Low-level jets in the NASA Ames Mars general circulation model, J. Geophys. Res., 102, 6511-6523.

Kraus, H., J. Malcher and E. Schaller, 1985: Nocturnal low-level jet during PUUK, Bound.-Layer Meteor., 31, 187-195.

Kulmala M., M. Lazaridis, A. Laaksonen, and T. Vesala: 1991: Extended hydrates interaction model: Hydrate formation and the energetics of binary homogeneous nucleation, J. Chem. Phys., 94, 7411-7413.

Kulmala M., V.-M. Kerminen and A. Laaksonen: 1995: Simulations on the effect of sulphuric acid formation on atmospheric aerosol concentrations. Atmos. Environ., 29, 377-382.

Lalas, D.P. and F. Einaudi, 1973: On the stability of a moist atmosphere in the presence of a background wind, J. Atmos. Sci., 30, 795-800.

Leck, C., E.D. Nilsson, K.E. Bigg and L. Backlin, 2001: Atmospheric program on the Arctic Ocean Expedition 1996 (AOE-96): An overview of scientific goals, experimental approach and instruments, J. Geophys. Res., 106, 32051-32067.

Liu, A.K. and D.O. ReVelle, 1992: Mesoscale spatial variability of nocturnal low-level jet winds, Paper 9.1, Preprints of the 5th Conference on Mesoscale Processes, Amer. Meteor. Soc., Boston, Mass., 307-312.

Malcher, J. and H. Krauss, 1983: Low-level jet phenomena described by an integrated dynamic PBL model, Bound.-Layer Meteor., 27, 327-343.

Miles, J., 1986: Richardson's criterion for the stability of stratified shear flow, Phys. of Fluids, 29, 3470-3471.

Nilsson, E.D., 1996: Planetary boundary layer structure and air mass transport during the International Arctic Ocean Expedition 1991, Tellus, 48B, 178-196.

Nilsson, E.D. and S. Barr, 2001: Effects of synoptic patterns on atmospheric chemistry and aerosols during the Arctic Ocean Expedition 1996, J. Geophys. Res., 106, 32069-32086.

Nilsson, E.D. and E. K. Bigg: 1996: Influences on

formation and dissipation of high arctic fogs during summer and autumn and their interaction with aerosol, Tellus, 48B, 234-253.
Nilsson, E.D. and Ü Rannik, 2001: Turbulent aerosol fluxes over the Arctic Ocean.: 1. Dry deposition over sea and pack ice, J. Geophys. Res, 106, 32125-32137.
Nilsson, E.D., Ü. Rannik and M. Håkansson, 2001: Surface Energy budget over the central Arctic Ocean during late summer and early freeze-up, J. Geophys. Res., 106, 32187-32205.
Nilsson, E.D. and D.O. ReVelle, 2003: Characteristics and dynamics of the low-level Jets over the central Arctic Ocean pack ice (To be submitted).
Parish, T.R., 2000: Forcing of the summertime low-level jet along the California coast, J. Appl. Meteor., 39, 2421-2433.
Pomeroy, K.R. and T. R. Parish, 2001: A case study of the interaction of the summertime coastal jet with the California topography, Month. Weath. Rev, 129, 530-539.
Poulos, G.S., W. Blumen, D.C. Fritts, J.K. Lundkuist, J. Sun, S.P. Burns, C. Nappo, R. Banta, R. Newsom, J. Cuxart, E. Terradellas, B. Balsley and M. Jensen, 2002: CASES-99: A comprehensive investigation of the stable nocturnal boundary layer, Bull. Amer. Meteor. Soc., 83, 555-581.
Ray, P.S., 1986: Mesoscale Meteorology and Forecasting, Amer. Meteor. Soc., Boston, 793 pp.
ReVelle, D.O., J.A. Logsdon and A.K. Liu, 1990: The low-level nocturnal jet phenomena: A diagnostic sensitivity study of the primary and secondary factors affecting its development and evolution, Paper 13.2, Preprints of the 4th AMS Conference on Mesoscale Processes, Amer. Meteor. Soc., Boston, Mass., 228 - 229.
ReVelle, D.O. and A.K. Liu, 1992: Some effects of synoptic-scale baroclinicity on Nocturnal PBL Jets, Paper 9.2, Preprints of the 5th Conference on Mesoscale Processes, Amer. Meteor. Soc., Boston, Mass., 313-318.
ReVelle, D.O., 1993: Chaos and bursting in the planetary boundary layer. J. Appl. Meteor., 32, 1169-1180.
ReVelle, D.O. and R.L. Coulter, 1994: Observations of the stable, nocturnal boundary layer: Minisodar analyses of intermittent breakdown events, Proceed. 7th Internat. Sympos. Acoustic Remote Sensing of Atmosphere and Ocean, NOAA-ETL, W. Neff, Ed., Boulder ISARS'94, 2-41-2-45.
ReVelle, D.O. and R.L. Coulter, 1995: Bursting in the near-surface boundary layer: Comparisons between realistic models and observations, Paper 17.1, Preprints of the 11th AMS Symposium on Boundary Layers and Turbulence, Amer. Meteor. Soc., Boston, Mass., 560-563.
ReVelle, D.O., E.D. Nilsson and M. Kulmala, 1997: Modeling of the Arctic boundary layer: Comparisons with measurements from the Arctic Ocean expedition 1996, Poster paper 6.6, Preprints of the 12th AMS Symposium on Boundary Layers and Turbulence, Amer. Meteor. Soc., Boston, Mass., 148-149.
ReVelle, D.O., 1997: On predicting the transition to turbulence in stably stratified fluids, Poster paper 6.7, Preprints of the 12th AMS Symposium on Boundary Layers and Turbulence, Amer. Meteor. Soc., Boston, Mass., 150-151 (The full paper is available at Los Alamos National Laboratory as LA-UR-97-1315).
Savijarvi, H., 1993: The Martian slope winds and the nocturnal PBL jet, J. Atmos. Sci., 50, 77-88.
Smedman, A.-S., M. Tlernstrom and U. Hogstrom, 1993: Analysis of the turbulence structure of a marine low-level jet, Bound.-Layer Meteor., 66, 105-126.
Sorbjan, Z., 1989: Structure of the Atmospheric Boundary Layer, Prentice Hall, Englewood Cliffs, N.J., 317 pp.
Stull, R.B., 1988: An Introduction to Boundary Layer Meteorology, Kluwer Academic Publishers, Dordrecht, The Netherlands, 666 pp.
Thorpe, A. J. and T. H. Guymer, 1977: The nocturnal jet, Quart. J. Roy. Meteor. Soc. 103, 633-653.
Van de Wiel, B. J. H., R. J. Ronda, A. F. Moene, H. A. R. De Bruin, and A. A. M. Holtslag, 2002a: Intermittent turbulence and oscillations in the stable boundary layer over land. Part I: A bulk model. J. Atmos. Sci., 59, 942–958.
Van de Wiel, B. J. H. , A. F. Moene, R. J. Ronda, H. A. R. De Bruin, and A. A. M. Holtslag 2002b: Intermittent turbulence and oscillations in the stable boundary layer over land. Part II: A system dynamics approach, J. Atmos. Sci., 59, pp. 2567–2581.
Van de Wiel, B. J. H., A. F. Moene, O. K. Hartogensis, H. A. R. De Bruin, and A. A. M. Holtslag, 2002c, Intermittent turbulence and oscillations in the stable boundary layer. Part III: A Classification for observations during CASES99. J. Atmos. Sci., In Press.